ELSEVIER

Thin Solid Films 270 (1995) 462–466

thin solid films

Selective tungsten CVD on submicron contact hole

Wen-Kuan Yeh [a], Mao-Chieh Chen [a], Pei-Jan Wang [b], Lu-Min Liu [b], Mou-Shiung Lin [b]

[a] *Department of Electronics Engineering, National Chiao Tung University and National Nano Device Laboratory, Hsinchu, Taiwan*
[b] *Taiwan Semiconductor Manufacturing Company, Hsinchu, Taiwan*

Abstract

This work investigates the deposition properties of selective chemically vapor-deposited tungsten for filling the deep sub-half micron contact holes using the process of silane reduction of tungsten hexafluoride. Low-resistivity tungsten with excellent selectivity and conformal coverage can be obtained with a SiH_4/WF_6 flow rate ratios less than 0.6 at deposition temperatures between 280 to 350 °C. Junction leakage and contact resistance of the AlSiCu/W/n^+p and AlSiCu/W/p^+n diodes as well as the electromigration properties of the AlSiCu/W/n^+p structure were investigated.

Keywords: Tungsten; Chemical vapour deposition; Contacts

1. Introduction

Selective tungsten chemical vapor deposition (W-CVD) is one of the most attractive techniques for filling deep submicron contact holes for ultra large scale integration (ULSI) applications. Selective W-CVD can be performed using hydrogen (H_2) reduction [1] or silane (SiH_4) reduction [2,3] of tungsten hexafluoride (WF_6).

Selective W-CVD using the H_2 reduction process suffers from high reactivity of WF_6 toward the silicon substrate. Thus, it causes excessive Si consumption, encroachment at the Si/SiO_2 interface, and worm-hole formation in the contact regions [4,5]. These disadvantages do not happen with the silane reduction process [6]. In the SiH_4 reduction process, the chemical reaction of the SiH_4/WF_6 system is rather complicated. The major problem of the selective W-CVD is the lack of control and understanding of the selectivity loss. It is generally acknowledged that the deposition temperature and reactant flow rate are two of the most important parameters for the deposition selectivity of the SiH_4/WF_6 chemistry. The W deposition conditions tend to influence the electrical characteristics of W-contacted shallow junctions. In addition, since little work has been done on the electromigration-induced failure of the W-filled contact holes with AlSiCu/W/Si structure, highly reliable selective W filling on deep submicron contact holes is of great concern if the technique is to be used in a ULSI process flow. This work investigates the deposition properties of selective W filling on submicron contact holes using the silane reduction process. The morphology and resistivity of W film were also investigated. Electrical characteristics of W-contacted n^+p and p^+n junction diodes were studied. In addition, electromigration-induced failure of the AlSiCu/W/n^+p junction structure was investigated.

2. Experimental details

The starting material was ⟨100⟩-oriented p-type Si wafers with 8–12 Ω cm nominal resistivity and n-type Si wafers with 10–20 Ω cm nominal resistivity. After RCA standard cleaning, the wafers were thermally oxidized to grow an oxide layer of 1500 Å thickness followed by a deposition of 4500 Å thickness of BPSG. Diffusion areas with sizes ranging from 200×200 to 1200×1200 μm^2 were defined using conventional photolithographic technique and reactive ion etching. For the p^+n junction, the junction implant was carried out by BF_2^+ implantation on the n-type substrate at 30 keV to a dose of 3×10^{15} cm^{-2} followed by furnace annealing at 900 °C for 30 min in N_2 ambient. For the n^+p junction, the junction implant was carried out by As^+ implantation on the p-type substrate at 50 keV to a dose of 5×10^{15} cm^{-2} followed by furnace annealing at 950 °C for 30 min in N_2 ambient. A 6000 Å thick layer of SiO_2 was then deposited on all the wafers using $TEOS/O_2$, and contact holes with sizes ranging from 0.35 to 5 μm were defined using conventional photolithographic technique and reactive ion etching. Prior to conducting the selective W-CVD, the wafers were dipped in dilute HF (2%) for 30 s followed by rinse in deionized water for 2 min. The wafers were then loaded into the load-locked cold

0040-6090/95/$09.50 © 1995 Elsevier Science S.A. All rights reserved
SSDI 0040-6090(95)06715-9

wall W-CVD system within 5 min. An in-situ predeposition plasma etching was conducted with the following conditions: r.f. power, 30 W; total gas pressure, 100 mTorr; NF_3 flow rate, 12 sccm; and N_2 flow rate, 72 sccm. After the plasma etching, the wafers were transferred from the plasma etching chamber to the tungsten deposition chamber without exposure to the atmosphere. The base pressure of the CVD chamber is 10^{-6} Torr. In this work, the W-CVD was conducted with conditions illustrated as follows: substrate temperature, 280–400 °C; total gas pressure, 100 mTorr; WF_6 flow rate, 20–30 sccm; SiH_4 flow rate, 10–20 sccm; and H_2 carrier gas flow rate, 0–1400 sccm. After the selective W-CVD, Al alloy metallization was applied followed by 30 min sintering at 400 °C.

The W-film thickness in the contact hole was determined by cross-sectional scanning electron microscopy (SEM). The resistivity of the W films was measured by a four-point probe. X-ray diffraction analysis (XRD) was used to identify the crystal type of the W film. The selectivity of W-CVD was examined by optical microscope in the dark-field mode. The contact resistance of W/n^+p and W/p^+n was measured using a four-terminal Kelvin structure as well as a contact chain structure. Electromigration-induced failure of the $AlSiCu/W/n^+p$ diode structure was detected using the contact chain structure. Contact chains used for the reliability test consisted of 100 contact holes with a contact size of 2 μm. In the electromigration test, the time to failure (TF) was defined as the time when the magnitude of contact resistance increased by 50%. In this work, stress current ranging from 0.75 to 1.5×10^6 A/cm^2 and sample temperature ranging from 225 to 275 °C were used for the electromigration test.

3. Results and discussion

The Arrhenius plot of W-CVD on the substrate with submicron contact holes is illustrated in Fig. 1. The process window for the selective deposition ranged from 280 to 350 °C with an activation energy of 0.84 eV. In this temperature

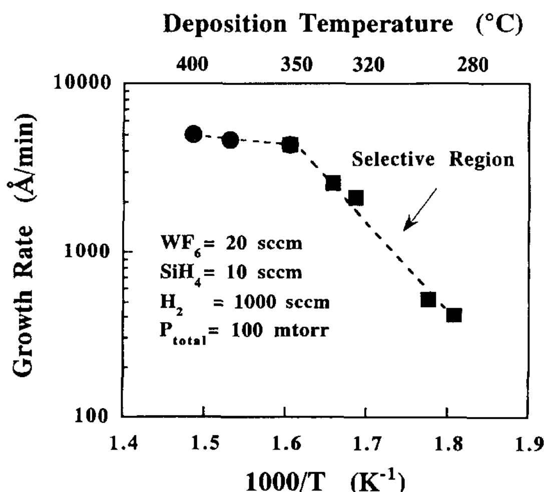

Fig. 1. Dependence of tungsten deposition rate on deposition temperature.

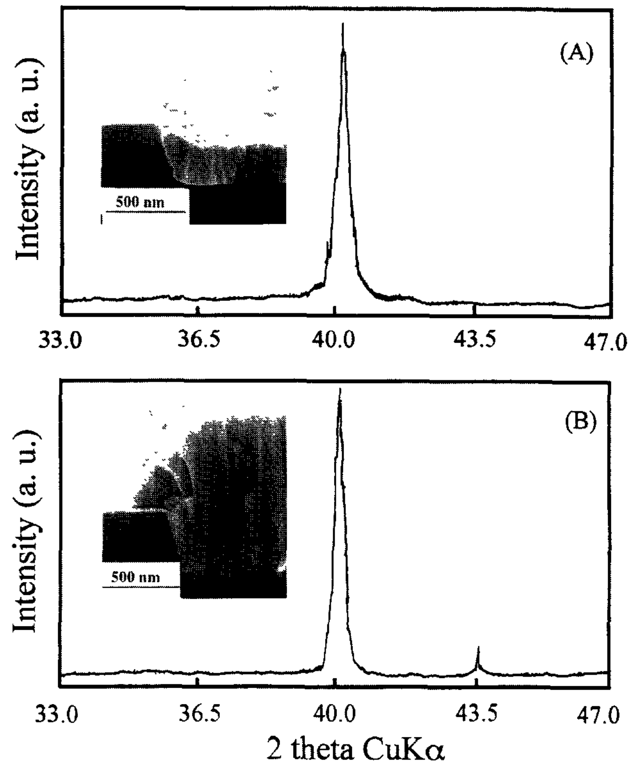

Fig. 2. XRD spectra of W films and cross-sectional SEM micrographs of W filling of contact holes with deposition temperature at (a) 300 °C and (b) 400 °C.

range, surface substitution reaction is the dominant process of W-CVD, which is controlled by the rate of diffusion of Si through the W film [7]. At temperatures higher than 350 °C, W film was deposited not only on the Si substrate but also along the sidewall of contact hole and on the SiO_2 surface leading to W selectivity loss. Tungsten was easily nucleated at the SiO_2 surface at high deposition temperatures because the reaction by-product SiF_2 reacts with WF_6 species resulting in W deposition on SiO_2 [8]. The W film deposited at 300 °C has a granular structure [9] with low resistivity (~ 12.5 μΩ cm), as shown in Fig. 2(a); in contrast, the film deposited at 400 °C has a columnar structure [9] with high resistivity (~400 μΩ cm), as shown in Fig. 2(b). Tungsten can be categorized into low-resistivity α-type ($\rho < 100$ μΩ cm) and high-resistivity β-type ($\rho > 300$ μΩ cm). The W film deposited at low temperature has a smoother surface morphology than that deposited at high temperature. In addition to a rougher surface, the thick W film deposited at high temperatures has large grain size as well as low selectivity. A high deposition temperature also enhanced the Si reduction process, causing larger consumption of Si and more severe encroachment at the Si/SiO_2 interface. In addition to the deposition temperature, the reactant flow rate is another important parameter for the resistivity of W films. The flow rate ratio of SiH_4/WF_6 was found to have a profound effect on the resistivity of the deposited W film. Fig. 3 shows the dependence of W film resistivity on the SiH_4/WF_6 flow rate ratio with various fixed flow rates of WF_6. At a deposition temperature of 300 °C, low-resistivity W films with granular

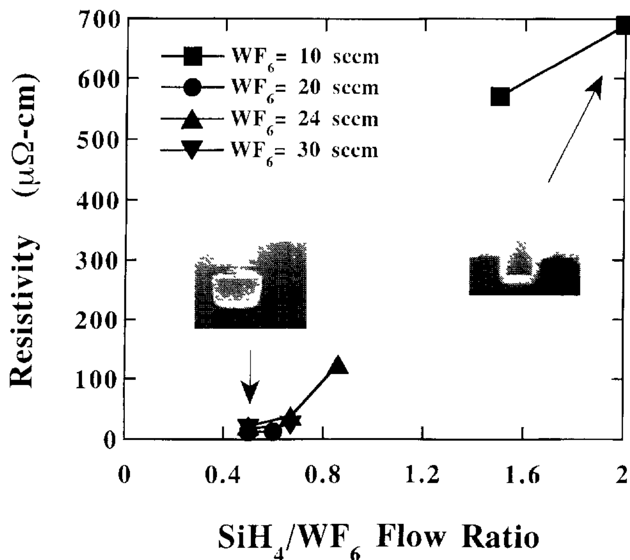

Fig. 3. Dependence of W film resistivity on flow rate ratio of SiH_4/WF_6 with various fixed flow rates of WF_6. The W films were deposited at 300 °C.

structure belonging to α-type can be selectively and conformally deposited on submicron contact holes with a low (< 0.6) SiH_4/WF_6 flow rate ratio. On the other hand, at high flow rate ratio of SiH_4/WF_6 (e.g. ratio of 2), high-resistivity W films with columnar structure presumably belonging to β-type was deposited not only on the Si substrate at the bottom of the contact hole but also along the sidewall of the contact hole leading to blanket deposition of W. For a SiH_4/WF_6 ratio less than 1, pure W of bulk density and resistivity can be deposited. On increasing the ratio to 2, nearly 40 at.% Si is incorporated in the films [10] and the metastable high-resistivity β-W phase is present [11]. Due to the high deposition rate of W (> 15000 Å min^{-1}) enhanced by increased SiH_4 partial pressure, W could not fill the submicron contact hole leading to void formation, as shown in Fig. 3. At a constant total pressure and fixed flow rates of WF_6 and SiH_4, the partial pressures of WF_6 and SiH_4 will increase with the lowering of carrier gas flow rate. Thus, at very low flow rates of carrier gas or no carrier gas at all, the increased partial pressures of WF_6 and SiH_4 would result in the deposition of W particles on the chamber wall of the W-CVD system and also lead to deposition selectivity loss and high-resistivity β-type film deposition. In this work, the flow rate of H_2 carrier gas must be controlled between 400 and 1400 sccm, and the total gas pressure ranging from 10 to 100 mTorr was used. Within the above-mentioned ranges of H_2 flow rate and total gas pressure, excellent selectivity (selectivity loss less than one per cm^2) was obtained within the process temperature window of 280 to 350 °C with a low flow rate ratio of SiH_4/WF_6 for W-CVD on a 0.35 μm contact hole patterned substrate, as shown in Fig. 4(a). Fig. 4(b) shows a cross-section SEM micrograph of W filling on a 0.35 μm contact hole with an aspect ratio of 2. Smooth W/Si interface as well as little Si consumption was obtained.

The current–voltage characteristics were investigated on W/p^+n and W/n^+p junction diodes fabricated by selective W-CVD. The diode's area was 10^{-2} cm^2, and at least 40 randomly chosen diodes were measured in each case. Fig. 5 illustrates the histograms showing the distribution of the reverse leakage current density measured at −5 V. The average reverse leakage current density is about 2 nA cm^{-2} for the W/p^+n junction diodes, while the leakage current density for the W/n^+p diodes was found to be more than one order of magnitude larger than that of the W/p^+n diodes. Two important features must be considered. First, the Si encroachment may still happen and extend thicker in n^+ junctions than p^+ junctions [12]. Second, much of the n^+ Si substrate surface was consumed as compared with the p^+ Si substrate surface during W-CVD, which increased reverse junction leakage for the W/n^+p shallow junction diodes [13]. The contact resistance was measured for the $AlSiCu/W/n^+p$ and $AlSiCu/W/p^+n$ junction diodes. For the $AlSiCu/W/n^+p$ diode with a contact area of 4 μm^2, the measured contact resistances were about 20 and 120 Ω, respectively, using a four-terminal Kelvin structure and a contact chain structure. The large contact resistance measured by the contact chain structure is due to the contribution from the n^+ diffusion layer. Fig. 6 shows the measured contact resistance versus contact size using the Kelvin structure. Contact resistivity of the $AlSiCu/W/p^+n$ diodes is about five times higher than that of the $AlSiCu/W/n^+p$ diodes ($\sim 3 \times 10^{-7}$ Ω cm^2); this

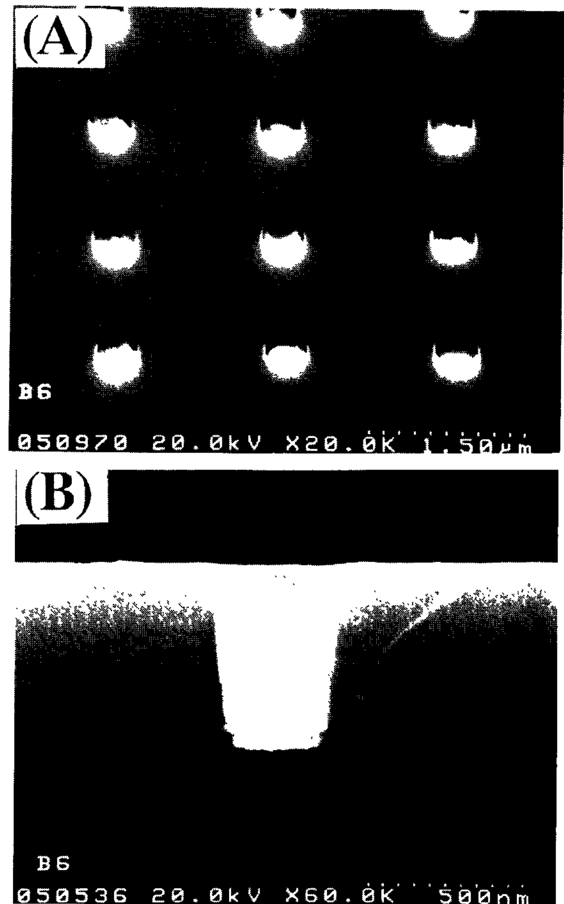

Fig. 4. (a) Top-view and (b) cross-section SEM micrographs showing selective W deposition in 0.35μm contact holes.

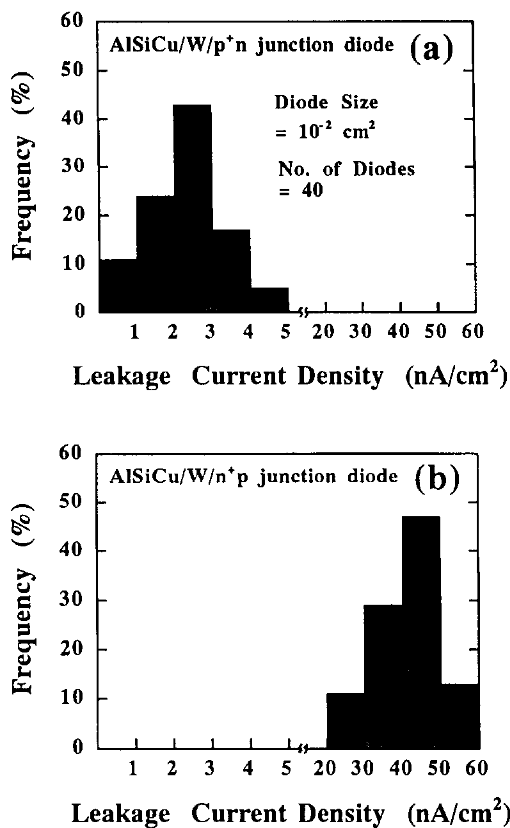

Fig. 5. Histograms showing the distribution of reverse leakage current density measured at −5 V for (a) AlSiCu/W/p$^+$n and (b) AlSiCu/W/n$^+$p junction diodes.

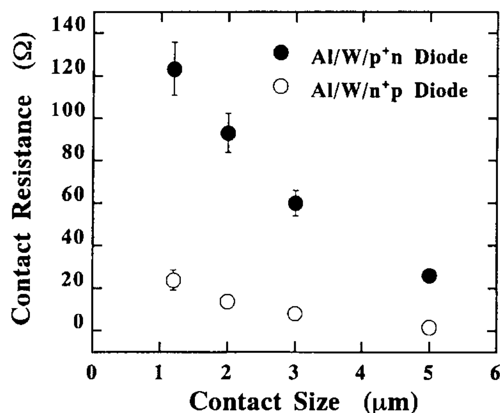

Fig. 6. Contact resistance versus contact size for the (a) AlSiCu/W/p$^+$n and (b) AlSiCu/W/n$^+$p diodes.

is presumably due to the fact that the As atoms are largely segregated at the W/Si interface [14].

Electromigration-induced failure for the AlSiCu/W/n$^+$p diode was investigated by measuring the temperature dependence of the time to failure (TF) for the tungsten-filled contact hole structure. Fig. 7 shows the Arrhenius plot obtained from measurement on contact chain structures with 2 μm contact size. The failure activation energy was determined to be 0.853 eV, which is higher than the reported value of 0.62 eV obtained from measurement on tungsten-filled via hole structure [15]. This value does not correspond to the activation energy for tungsten electromigration, which was estimated as 1.9 eV [15]. Rather, it corresponds closely to that of the aluminum grain boundary diffusion, which was reported to be 0.5–0.7 eV [16]. Fig. 8(a) shows the top-view SEM micrograph of the contact open failure. It is apparent that open failure occurred in the aluminum and not in the tungsten.

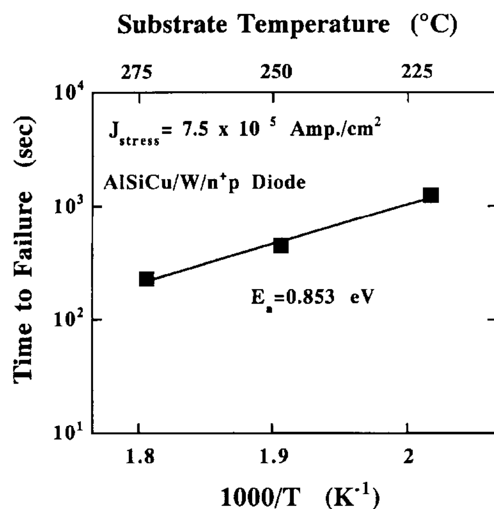

Fig. 7. Time to failure (TF) of the AlSiCu/W/n$^+$p diode versus substrate temperature.

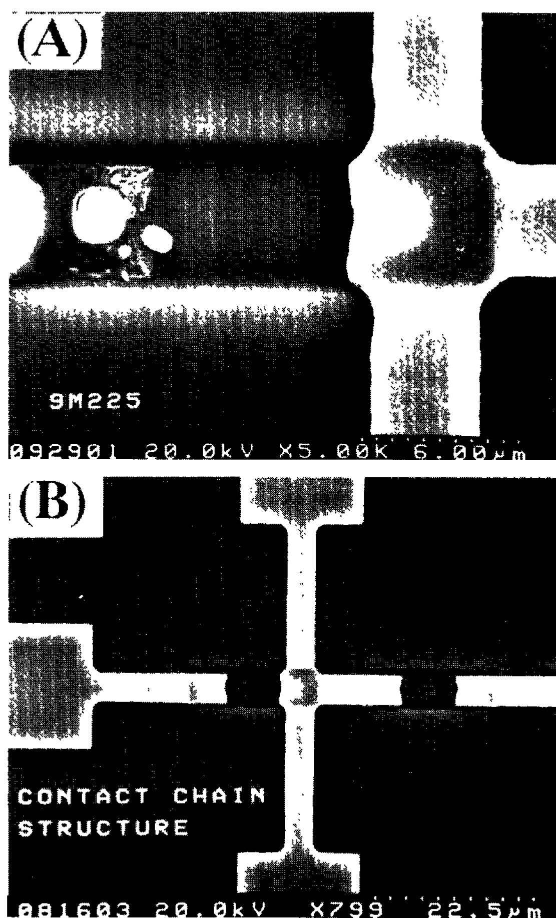

Fig. 8. SEM micrographs showing (a) electromigration-induced failure of the AlSiCu/W/n$^+$p diode with a stress current of 9×10^5 A cm^{-2} at a substrate temperature of 225 °C, and (b) the AlSiCu/W/n$^+$p diode before the current stress.

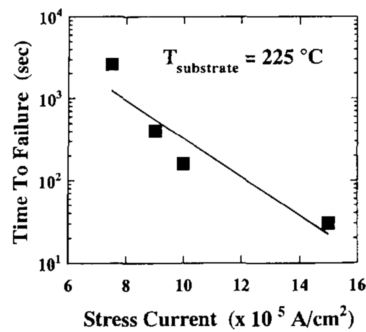

Fig. 9. Time to failure (TF) of the AlSiCu/W/n^+p diode versus stress current density.

Compared with the sample before current stress and substrate heating (as shown in Fig. 8(b)), it is apparent that the failure mechanism of contact migration for the AlSiCu/W/n^+p structure is due to aluminum grain boundary diffusion by which the aluminum atoms migrated from the W-filled contact hole along the direction of electron flow, leading to the exposure of W surface. Contact migration of AlSiCu/W/n^+p structure did not occur with opposite bias current stress (negative bias was connected to aluminum pad), which would cause aluminum to be segregated at aluminum pad around the W-filled contact hole. Stress current is another factor in electromigration failure of this metallization system. Fig. 9 shows the dependence of TF on the stress current density. A high current density causes joule heating leading to the stress-induced failure of contact chain.

4. Conclusion

The processing window of selective W-CVD using the SiH_4 reduction process was determined to be: substrate temperature, 280–350 °C; total gas pressure, 10–100 mTorr; flow rate ratio of SiH_4/WF_6, <0.6; and H_2 carrier gas flow rate, 400–1400 sccm. Low-resistivity W films with excellent selectivity and coverage in deep sub-half micron contact holes with aspect ratio of 2 can be obtained. For tungsten contacted shallow junctions, thicker encroachment and larger Si consumption on the n^+p substrate results in larger junction leakage for the W/n^+p diode than the W/p^+n diode. Contact resistance of the AlSiCu/W/n^+p diode was about five times lower than that of the AlSiCu/W/p^+n diode, possibly due to large segregation of arsenic atoms at the W/Si interface. Contact electromigration lifetime is limited by the migration of aluminum away from the W-filled contact holes along the direction of electron flow.

Acknowledgements

This work was supported by the National Science Council (ROC) under contract no. NSC84-2622-E009-007-1.

References

[1] C.M. McConica and K. Krishnamani, *J. Electrochem. Soc., 133* (1986) 2542.
[2] R.F. Foster, S. Tseng, L. Lane and K.Y. Ahn, *Tungsten Workshop III*, MRS, New York, 1988, p. 69.
[3] Y. Kusumoto, K. Takakuwa, H. Hashinokuchi, T. Ikuta and I. Nakayama, *Tungsten Workshop III*, MRS, New York, 1987, p. 103.
[4] W.T. Stacy, E.K. Broadbent and M.H. Norcott, *J. Electrochem. Soc., 132* (1985) 444.
[5] R.A. Levy, M.L. Green, P.K. Gallagher and Y.S. Ali, *J. Electrochem. Soc., 133* (1986) 1905.
[6] R.S. Rosler, J. Mendonca and M.J. Rice, Jr., *J. Vac. Sci. Technol., B6* (1988) 1721.
[7] R.V. Joshi, V. Prasad, L.K. Elbaum, M. Yu and M. Norcott, *J. Appl. Phys., 68* (1990) 5625.
[8] R. Roster, L. Lane and S. Tseng, *Tungsten Workshop III*, MRS, New York, 1988, p. 159.
[9] T.I. Kamins, D.R. Broadbury, T.R. Cass, S.S. Laderman and G.A. Reid, *J. Electrochem. Soc., 133* (1986) 2555.
[10] V.V.S. Rana, M. Eizenberg, S. Ghanayen, J. Roberts and A.K. Sinha, *MRS Symp. Proc., 337* (1994) 569.
[11] C.C. Tang and D.W. Hess, *Appl. Phys. Lett., 45* (1984) 633.
[12] C. Yang and J. Multani, *Proc. VMIC*, Santa Clara, 1987, p. 200.
[13] H. Itoh, N. Kaji, T. Watanabe and H. Okano, *Jpn. J. Appl. Phys., 40* (1991) 1525.
[14] B.Y. Tusi and M.C. Chen, *Solid State Electron., 35* (1992) 1217.
[15] F. Matsuoka, H. Iwai, K. Hama, H. Itoh, R. Nakata, T. Nakakubo, K. Maeguchi and K. Koazaki, *IEEE Trans. Electron. Dev., ED-37* (1990) 562.
[16] M.J, Attarado and R. Rosenberg, *J. Appl. Phys., 41* (1970) 2381.